Available online at www.sciencedirect.com
ScienceDirect
Journal of Nuclear Materials 363–365 (2007) 1081–1086
journal of nuclear materials
www.elsevier.com/locate/jnucmat

ELM induced carbon contamination of ITER core

S. Pestchanyi *, I. Landman

Forschungszentrum Karlsruhe, Institute for Pulsed Power and Microwave Technology, P.B. 3640, D-76021 Karlsruhe, Germany

Abstract

Type I ELMs in ITER would result in the divertor targets vaporization. Vaporized carbon plasma can contaminate the thermonuclear plasma in the ITER core decreasing the plasma temperature and the fusion power or even run the confinement into disruption. Simulations of the tolerable ELM frequency as a function of ELM size are carried out for ITER using TOKES and FOREV-2D codes. Improved FOREV-2D scenario proposed for simulation of the carbon plasma influx into ITER pedestal. An elaborated model for carbon penetration into the confined plasma from pedestal is implemented in TOKES. Simulation of tolerable ELM frequency has been done for 3.5–12.1 MJ of the total ELM energy loss. The tolerable frequency is less than 10 Hz for the ELM of 7.3 MJ and decreases with increasing of the energy loss.

PACS: 28.52.−s; 52.55.−s; 52.55.Dy; 52.55.Fa

Keywords: ELM; Carbon contamination; Cross-field diffusion; SOL transport modeling; Radiation loss

1. Introduction

ELMy H-mode is the operational scenario foreseen for the future tokamak reactor ITER. However, this regime associates with a heat flux at the carbon fibre composite (CFC) divertor armour during ELMs of 2–3 orders of magnitude over its background value. Modern tokamaks do not produce ELMs powerful enough to cause vaporization at the divertor surface, except of very special regimes in JET, but type I ELMs anticipated in ITER would dump up to 1–4 MJ/m^2 onto the armour during 0.1–0.5 ms, which results in the vaporization. After such an ELM the carbon plasma fills the scrape-off layer (SOL) with density varying between 10^{21} and 10^{20} m^{-3} [1]. Carbon ions having penetrated after the ELM into the periphery of confinement region diffuse into the core and re-radiate electron thermal energy from the whole plasma volume.

Estimations made in [1,2] have been done by the two-dimensional radiation MHD code FOREV-2D and the code TOKES for only one carbon inflow $N_c = 2.25 \times 10^{20}$, with a conclusion that a tolerable ELM energy at this inflow corresponds to ELM repetition period 2 s. For this estimation rather simplified FOREV scenario has been developed. The scenario assumes that hot deuterium–tritium plasma of the pedestal region looses through the separatrix with a constant loss rate and then it appears in SOL having constant temperature and exponential

* Corresponding author.
E-mail address: serguei.pestchanyi@ihm.fzk.de (S. Pestchanyi).

0022-3115/$ - see front matter © 2007 Elsevier B.V. All rights reserved.
doi:10.1016/j.jnucmat.2007.01.234

distribution of the density across SOL. The cross diffusion of DT and carbon plasmas was not taken into account. Using the scenario FOREV simulated CFC armour vaporization at the armour surface under influence of hot plasma transported from the pedestal during ELM. The estimations performed have shown the order of the magnitude for the amount of contamination plasma in SOL using reasonable assumption for the hot plasma profile across SOL. However, the armour vaporization rate is strongly dependent on the details of the power flux induced by ELM. Type I ELM energies cover the interval, which includes the vaporization threshold inside. This means that smaller ELMs would not cause armour vaporization, but ELMs with energy under the threshold will do. The amount of vaporized target material is a strong and nonlinear function of the deposited energy. The vaporization threshold and vaporized mass are dependent not only on the mean heat load and the ELM time duration, but rather on its peaking on divertor and on the time dependence.

These arguments motivated for more realistic simulation of the divertor power load during ELMs. Self-consistent simulation of ELM is a challenge for modern computational plasma physics. FOREV-2D is not suited for such simulation. Instead, it uses a phenomenological scenario, setting up the ELM parameters, needed for simulation of divertor targets vaporization and ionisation of the vapour. In the present work the phenomenological ELM scenario is significantly improved in comparison with the simulation, done in [1]. It does not prescribe the power density profile and the constant power flux to SOL. Both, power flux profile at the divertor and its time dependence are calculated, using the plasma transport equations along and across the stationary magnetic field and the simplifying assumption on the plasma diffusion coefficient.

New simulations of the tolerable ELM frequency as a function of ELM size are carried out using TOKES code for the carbon influxes obtained from FOREV-2D simulations. An elaborated model for carbon penetration into the confined plasma is now implemented in TOKES. The carbon ions diffuse across all other species of the fusion reactor: deuterium D, tritium T and He. The plasma boundary region can accept arbitrary large post-ELM contamination, even if the carbon density n_C exceeds the main species densities. The radiation losses are calculated as earlier, based on the Post's calculations.

2. FOREV-2 scenario for ELM

To simulate ELMs in ITER using the data measured at modern tokamaks and extrapolated to ITER (see [3–5]) it was assumed that the divertor targets heat load during ELM is due to temporal enhancement of cross diffusion in pedestal and SOL. The adjusting parameters of the model – plasma diffusion coefficients – are fitted to reproduce the parameters measured at JET and DIII-D tokamaks and scaled to ITER. The time dependences for the temporal enhancement of ions/electrons diffusivities are assumed to be the same. Measured hot DT plasma flux behaviour is reproduced in the FOREV simulation by temporal increase of the diffusion coefficients in pedestal and SOL. The scenario used provides two adjusting parameters, D_{ped} – the diffusion coefficients in pedestal and D_{SOL} – the diffusion coefficients in SOL. It is assumed that $D_{ped}(t,y)$ and $D_{SOL}(t,y)$ are the values, dependent on time and on the position y along poloidal section of tokamak only. $D_{ped}(t,y)$ controls the amount of DT plasma, injected inside SOL during ELM. $D_{SOL}(t,y)$ controls cross diffusion for ELM plasma during transport in SOL and the heat load distribution between the first wall and the divertor. Both $D_{ped}(t,y)$ and $D_{SOL}(t,y)$ are fitted to reach their maxima at the outer midplane and drop to inner torus midplane. This variation of the diffusion coefficients reflects the fact that the outer midplane is the most unstable tokamak region for MHD instabilities. Time dependence of D_{ped}, D_{SOL} and of the heat fluxes to the divertor targets are shown in Fig. 1. The diffusion coefficients are not a measurable values, in our model they are fitted in size and in halfwidth τ_D for time dependence to ensure the ELM size and time dependence (halfwidth τ_{hf}) of the heat fluxes to the targets, which was measured and their scalings to ITER are available.

The heat flux to the divertor measured in JET does not cause target vaporisation. To ensure an accurate extrapolation of the flux to ITER the FOREV calculations has been done for ITER ELM parameters, but without targets vaporisation. These calculations specify the time dependence of the flux and the ELM size for specific choice of D_{ped}, D_{SOL} and their time dependence. Then, the calculations were repeated with the same $D_{ped}(t,y)$ and $D_{SOL}(t,y)$ but with targets vaporisation. Account of target vaporization reduces their heat loads due to shielding by the vaporized material, but the ELM parameters are already known.

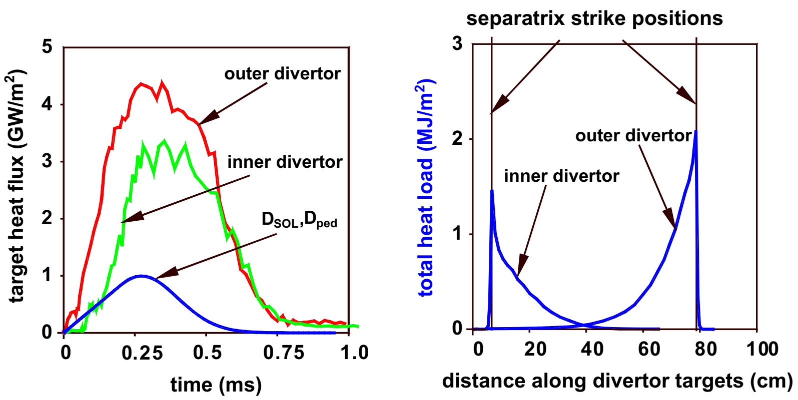

Fig. 1. In the left panel the time dependence $D_{ped}(t)$ is shown in arbitrary units together with the heat fluxes at outer and inner divertor SSPs due to this additional diffusion. $D_{SOL}(t)$ has the same shape as $D_{ped}(t)$, but with the amplitude providing the heat flux of halfwidth 10–20 cm at the divertor targets as is seen from the right panel. The right panel combines in one plot the total heat loads of the inner and the outer targets during ELM of 12 MJ size and 0.5 ms time duration. Both heat fluxes are peaked at the corresponding SSPs, steeply drops to the private direction and gradually decrease in opposite direction.

3. Carbon diffusion simulation using TOKES

The TOKES code simulates diffusion of different ions in ITER magnetic configuration and radiation cooling rate during whole time of discharge. Using TOKES the magnetic configuration of reference ITER design was created and then fixed. The plasma temperature is given equal for all plasma species, dropping as the parabolic dependence of the poloidal magnetic flux from 12 keV at the magnetic axis $\mathbf{r}_0$ to 7 keV at the plasma boundary, which in carbon-free plasma corresponds to the α-fusion power of 80–90 MW. Plasma contamination by He and C decreases the fusion power and increases the radiation losses. The radiation flux varies between the ELMs significantly, with a sharp short increase just after the carbon injection and then decreases to the sustained inter-ELM value. Except for the sharp radiation increase, the total power loss due to ELM is approximately the sum of the inter-ELM radiation loss and the magnitude of fusion power drop caused by the carbon. The tolerable ELM repetition period is assumed to correspond to the total power loss below some threshold value, which is determined by technological and economical requirements. For our estimations the threshold value was rather arbitrary taken as half of the fusion power, namely 40 MW. Decrease of the threshold increases the tolerable ELM repetition period. The TOKES simulation starts from initially pure DT plasma, with the fusion reaction for producing He switched on and with a stationary fuelling that provides homogeneous sources of D (50%) and T (50%). The plasma diffusion coefficient is assumed be proportional to the square of electron density n_e, being equal 0.5 m²/s at the centre where the fuelling rate is adjusted to $n_e(\mathbf{r}_0) = 10^{20}$ m^{-3}. This modelling dependence of the plasma diffusion coefficient is enough for estimation of the core contamination and chosen because it provides reasonable density profile with the pedestal. Within a time period of a few seconds a stationary process establishes, however interrupted periodically with period τ by instantaneous injections of N_C carbon ions into the last plasma layer at the periphery. Cross transport of ion species is simulated with a classical ion–ion collisional frequency multiplied by a factor $F = 3$ that accounts for anomalous effects.

For ion species i (and j, i,j = D, T, He and C) the following equation is solved (in addition to a common diffusion equation of plasma itself which is not addressed in this work):

$$\frac{\partial n_i}{\partial t} = \frac{\partial}{\partial V}\left(\frac{1}{Z_i}\sum_{j\neq i}\left(Fc_{ij}\left(\frac{n_j}{Z_i}\frac{\partial p_i}{\partial V} - \frac{n_i}{Z_j}\frac{\partial p_j}{\partial V}\right)\right)\right). \quad (1)$$

Here t is time, V the inner volume of magnetic surfaces, p_i and Z_i species partial pressure and ion charge state, respectively, c_{ij} the transport constant ($c_{ij} = c_{ji}$) that includes a complicated Pfirsch–Schlüter geometric factor and the ion–ion collision frequency.

4. Simulation results

Results of the divertor heat load calculation without vaporization are shown in Fig. 1. The diffusion coefficients are fitted to ensure τ_{hf} of ~500 μs. Power fluxes to the targets are time and position dependent. The DT plasma density maximum is shifted from the separatrix due to the cross diffusion. However, the temperature profiles are peaked at the separatrix because longitudinal energy transport by electrons is faster than the electrons cross diffusion with D and T ions. As a result, the heat fluxes to the targets are peaked at the separatrix strike positions (SSP). Fig. 1 shows an integral heat load of both targets over whole ELM time.

Simulation of SOL contamination by carbon plasma has been done for 3.5 MJ, 4.0 MJ, 7.3 MJ, 9.7 MJ and 12.1 MJ total ELM energies. The results are listed in the Table 1. ELM of 3.5 MJ does not cause targets vaporisation, it starts at 4.0 MJ ELM size. Numbers of carbon atoms, vaporized from both divertor targets are listed in the Table 1. Approximately 10% of the vaporized carbon transported to SOL and covers the core of ITER by carbon plasma layer of $n_C = 10^{20}$–10^{21} m^{-3} density, depending on the ELM size. The layer thickness varies around $d = 2$–3 cm except of small regions close to x-points, where the thickness is of 10–20 cm. The carbon plasma density profiles across and along SOL for the ELM of 12.1 MJ size are plotted in Fig. 2. The FOREV simulations, performed till 1–2 ms after the ELM start, have shown rather uniform density distribution along SOL at that time. Few milliseconds after ELM the plasma temperature in SOL drops to 1–2 eV in the simulations with radiation cooling or to approximately ~30 eV with the radiation switched off. Estimations for the plasma on longer time indicate that free expansion with sound velocity along the magnetic field line of $L = 60$ m length between the divertor targets gives 15 ms living time in SOL for the plasma of temperature of 1 eV and 3 ms for 30 eV plasma.

Table 1
Numbers of carbon atoms, vaporized from both divertor targets

Total ELM energy (MJ)	Carbon atoms number	
	Vaporized	In SOL
3.46	0	0
4.83	Few	Few
7.33	6.6×10^{21}	4.9×10^{20}
9.73	3.5×10^{22}	2.8×10^{21}
12.1	2.3×10^{23}	1.7×10^{22}

The carbon plasma temperature in SOL is determined by electron heat conductivity and radiation cooling. Electron heat conductivity effectively cools down the plasma to the temperature of ~30 eV. Further cooling needs time larger than plasma living time in SOL, but radiative cooling of the plasma becomes more effective because of the radiation cooling barrier at ~10 eV for carbon plasma. Accurate estimation of the radiation cooling rate needs rather fine opacity data and therefore large calculation time. Our simulations performed with rather rough opacities was not accurate enough to make a conclusion whether the carbon plasma final temperature is of 1–2 eV or of ~30 eV, but estimation of carbon penetration inside the core has been done for both cases.

For the SOL carbon plasma of density n and temperature T, the gyro-radius of carbon ions in

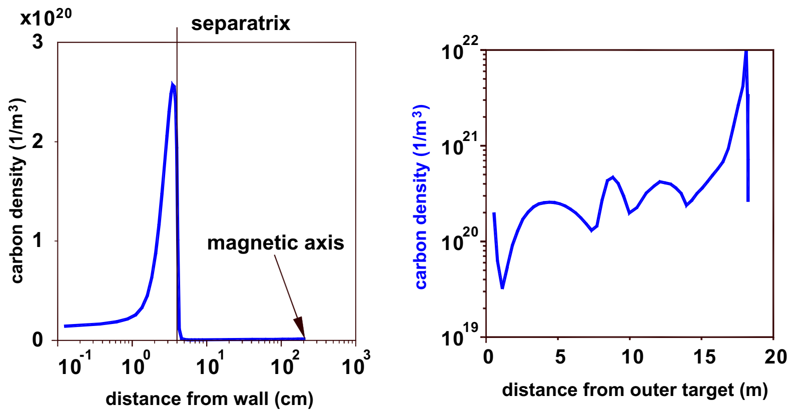

Fig. 2. Carbon plasma density profile along the ITER minor radius from wall to the magnetic axis at the distance of 5 m from the outer divertor target and the profile of maximal density along SOL. Shown the profiles at 1.1 ms after start of ELM of 12.1 MJ total energy and 0.5 ms time duration.

the magnetic field B is of $\rho = \sqrt{2}\frac{v_T m}{zeB}$ and their collision frequency $v = \frac{e^4 z^4 n \ln(\Lambda)}{12\sqrt{\pi^3 m T^3 \varepsilon_0^2}}$. During living time $\tau = \frac{L}{v_T}$ for carbon plasma in SOL the diffusion coefficient $D = \rho^2 v$ for the plasma provides estimation for carbon influx to the core: $j_C = \tau D \frac{n}{d} = 1.4 \cdot 10^{-21} \frac{z^2 n^2}{T\ (\mathrm{eV})}$ (m^{-2}) or, at least approximately half of the carbon in SOL, if it is less then the integral carbon influx through the separatrix. Comparison of the estimation with the values given in the Table 1 proves that for all the ELMs simulated the pedestal is contaminated by approximately half of the carbon in SOL. Using the data calculated by FOREV, the core contamination by carbon after multiple ELMs is calculated with the plasma equilibrium code TOKES. Carbon plasma diffusion inside the core is simulated for the whole ITER discharge.

The results of a numerical calculation for n_C using TOKES demonstrates Fig. 3 in which the propagation of the carbon impurity through the confined DT plasma after the first injection of the amount $N_C = 2.45 \times 10^{20}$ is shown. At each injection the time step value was abruptly decreased to 10^{-5} s, then incrementing by 10% each time step until reaching 10^{-1} s and then fixed, which allowed a proper calculation of the whole scenario with the drastically different time scales. The repetitive ELMs produce more and more plasma in the bulk, but due to simultaneous entrainment of carbon ions with the diffusive plasma the core carbon density and thus the carbon caused radiation loss power

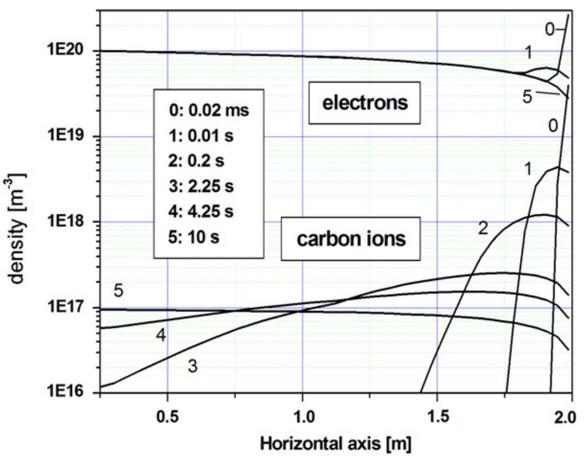

Fig. 3. Densities of electrons and carbon ions of post-ELM confined plasma as functions of horizontal Euclidian coordinate originated at the magnetic axis $\mathbf{r}_0$ at different time moments after ELM are shown. Carbon ions penetrate in the core during one second and then are entrained with the diffusing plasma back to the periphery.

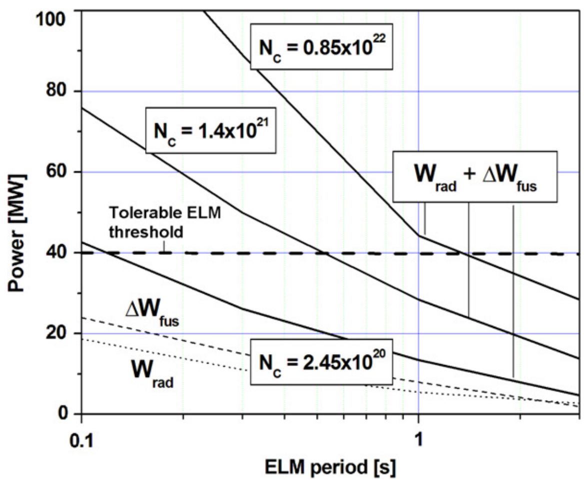

Fig. 4. The radiation and fusion power losses in the core plasma after injection of different amounts of carbon atoms into the periphery of confinement region due to ELM as a function of the ELM period.

gradually saturate at some value and the fusion power as well. The mentioned sustained inter-ELM radiation power loss W_{rad} and the fusion power drop ΔW_{fus} are shown in Fig. 4 for the case of $N_C = 2.45 \times 10^{20}$ and the sums $W_{\mathrm{rad}} + \Delta W_{\mathrm{fus}}$ for all cases.

Comparing the obtained tolerable ELM energy reached at $\tau > 0.1$ s for $N_C = 2.45 \times 10^{20}$ with that of [2] ($\tau > 2$ s) for approximately the same value of N_C we see a large difference, which is now interpreted as the consequence of the fact that in [2] the entrainment effect was not taken into account, thus the cleaning of plasma from the impurity was significantly slowed down in [2]. However, in terms of the ELM size the new result looks surprisingly similar, because the conclusion of [2] was that the tolerable ELM size of 1 MJ/m^2 corresponds to $\tau > 2$ s, and here we see that the averaged load onto a divertor is equal to 0.8–1.1 MJ/m^2 for $N_C = 0.85 \times 10^{22}$ for which we see the tolerable period is $\tau > 1.5$ s. In any case, our conclusion remains that the non-tolerable ELM sizes are roughly above 1 MJ/m^2.

5. Conclusions

Carbon ions having penetrated after type I ELM into the periphery of confinement region re-radiates the electron thermal energy decreasing the plasma temperature and the fusion power. Simulations of the tolerable ELM frequency as a function of ELM size are carried out using TOKES and

FOREV-2D codes. Improved FOREV-2D scenario proposed for simulation of the carbon plasma influx into ITER pedestal. An elaborated model for carbon penetration into the confined plasma from pedestal is now implemented in TOKES. The radiation losses are calculated based on the Post's calculations. Simulation of tolerable ELM frequency has been done for 3.5–12.1 MJ total ELM energies. The tolerable frequency is less than 10 Hz for the ELM of 7.3 MJ and decreases with increasing of the energy loss as is seen from Fig. 4. Extrapolation of type I ELM size from JET predicts ELMs up to 25 MJ in ITER, so the simulations should be continued to cover all the ITER ELM sizes.

Combination of FOREV-2D and TOKES codes is a proper tool for estimation of core plasma contamination after ELMs in various tokamaks. However, for more accurate predictions of the carbon plasma temperature and the ion charge states in SOL the opacity data for radiation transport in FOREV-2D code needs to be improved.

Acknowledgements

This work, supported by the European Communities under the contract of Association between EURATOM and Forschungszentrum Karlsruhe, was carried out within the framework of the European Fusion Development Agreement. The views and opinions expressed herein do not necessarily reflect those of the European Commission.

References

[1] S. Pestchanyi, B. Bazylev, I. Landman, Radiation losses from ITER SOL due to divertor material plasma. 31st EPS Conference on Plasma Phys. London, 28 June–2 July 2004 ECA vol. 28G, P-1.135, 2004.
[2] I.S. Landman, G. Janeschitz, in: 32nd EPS Conf. on Plasma Physics, Tarragona, Spain, June 27–July 1, 2005, P-1.003.
[3] A. Loarte et al., Plasma Phys. Control. Fusion 45 (2003) 1549.
[4] A. Loarte et al., Plasma Phys. Control. Fusion 44 (2002) 1815.
[5] J.A. Boedo et al., J. Nucl. Mater. 337–339 (2005) 771.